Damping in Civil Engineering Using SMA. The Fatigue Behavior and Stability of CuAlBe and NiTi Alloys

V. Torra, A. Isalgue, C. Auguet, G. Carreras, F.C. Lovey, H. Soul, and P. Terriault

Two types of application in damping of structures by SMA in Civil Engineering are considered. The first one is related to the reduction of the damage produced by earthquakes. The second one is concerned with the increase of the lifetime of the stayed cables in bridges. The analyses of the experimental conditions required for each application are different: Several years or decades without any activity (excepted the summer-winter room temperature parasitic effects) followed by one or two minutes of oscillations under the earthquake affects, or near 100000 oscillations per day with pauses of several hours or days in the damping of stayed cables in bridges. This article analyzes the fatigue behavior of the CuAlBe alloy (appropriate for earthquakes) and of the NiTi alloy. Measurements of the damping of stayed cables indicate that the oscillation amplitude could be reduced up to one-third by using a NiTi wire as a damper device.

1. Introduction

Shape Memory Alloys (SMAs) show particular properties associated to their martensitic transformation between metastable phases. The pseudoelasticity and thermoelasticity are effects related to their phase transition, used in sensors and actuators. The transformation often referred as a first-order phase transition with latent heat, shows hysteresis provided by different irreversible phenomena, i.e., when the interface overcomes internal barriers associated to dislocations (or arrays of dislocations, grain boundaries, and precipitates) (Ref 1).

The hysteretic behavior in this solid-solid transformation can be used in damping applications via the passive action of a structural component built in SMA by the conversion of mechanical energy to heat without hydraulic devices and/or external active or semi-active control (Ref 2). The active control requires expensive structures and external power supply that suppress the oscillations. The semi-active control requires sensors and actuators (i.e., as magneto-rheological fluids), appropriate computing systems and, also, a power supply

V. Torra, A. Isalgue, C. Auguet, and **G. Carreras**, CIRG-DFA-ETSECCPB, Polytechnical University of Catalonia, Gran Capita s/n, CAMPUS NORD B-4, 08034 Barcelona, Catalonia, Spain; **F.C. Lovey** and **H. Soul**, División Metales, Centro Atomico Bariloche and Instituto Balseiro, Avenida Bustillo 9500, Bariloche 8400, Argentina; and **P. Terriault**, Mechanical Engineering, Ecole de technologie superieure, 1100, Notre-Dame Street West, Montreal, QC H3C 1K3, Canada. Contact e-mail: vtorra@fa.upc.edu.

without stops (ensuring a quick run for the 365/365 days) useful in skyscraper, but usually difficult in free surrounding structures (i.e., bridges in the wilderness) under the direct action of external storms, which can generate, by electric sparks (lightning) in a thundercloud, spontaneous power failures. High-rise buildings are also vulnerable to hurricane-force winds, particularly at the higher levels, since wind speed tends to increase with height (Ref 3).

Many papers and reviews (Ref 4, 5) have been on the application of SMA's as damping devices in civil engineering, but they are difficult to apply because the behavior of the alloys is not carefully analyzed. In particular, the summer-winter temperature effects, self-heating, or residual strains requirements for the given applications are rarely well established. The use of SMA dampers requires a deep knowledge of SMA properties and their coherence with the application with clear explicit and/or implicit requirements (Ref 6). For instance, in earthquake engineering, the available experimental conditions shows that, after several years or decades at rest, i.e., without any oscillation, the damper is required to show an excellent behavior in one or two minutes of destructive activity (i.e., for structural frequencies around 1 Hz close or under 200 oscillations). The long duration at rest conditions supposes that the SMA does not show relevant diffusive effects. In particular, the mechanical analysis of the energetic conversion, from mechanical energy to heat, suggests the advantages of prestressed SMA (Ref 7). The use of Cu-based alloys after several years of prestressing can modify the thermomechanical behavior of the alloy via the martensite stabilization producing negative results during (and after) the earthquake. However, the prestressing is mechanically advantageous. It is also suggested the use of clamps, in the damper, reducing the length of the SMA wire in the "compressive part". Also, other diffusion effects need to be studied and quantified for these applications after extremely larger initial pauses (Ref 8, 9).

The Fig. 1 shows one of the targets in Civil Engineering: the damping of stayed cables in bridges. The Fig. 1(a) shows an outline of the Iroise bridge with stayed cables situated in the Elorn River (near Brest, France). Damping the cables'
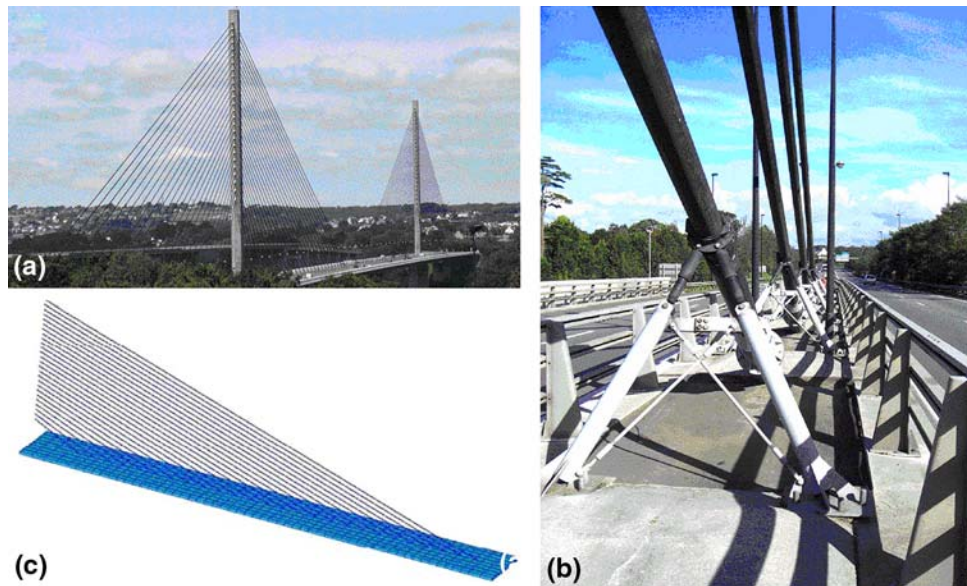
Fig. 1 (a) Highway bridge ("pont de l'Iroise" between Brest and Plougastel, France), platform: 200 + 400 + 200 m (length) 2 + 2 lanes. (b) Link of the cables to platform with two short hydraulic dampers. (c) Outline of the basic structure for simulation (one quarter of the bridge)

oscillation induced by wind and rain is of great technological importance. The Fig. 1(b) outlines the fixation of the cables to the platform (freeway with 2 + 2 lanes). The Fig. 1(c) shows a schema of the representative model used with dampers situated between stayed cables and platform.

In damping of earthquakes only, several minutes of working are required for one earthquake and replicas acting in a family house. The SMA dampers are situated in the diagonals of selected porticos. The situation is completely different when the target is the damping of stayed cables in bridges under the wind or rain effects. The cable frequencies are, for instance, close to 1-2 Hz (or more) and a large number of oscillations (100000) are expected for each day of work (with strong wind as in big storms). At this level, the damper can work "immediately" (or a few days) after installation without relevant initial quiet conditions (several years or decades) as in dampers used for family houses in earthquakes. In this situation, the initial time effects are extremely reduced and the useful working conditions are mainly controlled by the fatigue life. These conditions suggest that the prestressed material is probably a tool for an increased work. The more adequate analysis of these dampers relates to a deep study of the fatigue life and, eventually, positive ideas toward a practical increasing of the fatigue life of the material and the effect of pauses between series of oscillations, i.e., related to calm in the external wind/rain. In these applications (damping of seismic action effects or damping of stayed cable vibration) the SMA material is not allowed to increase significantly its length at working (Ref 10). However, all of the SMAs show some increase of length in cycling. This phenomenon always requires a particular study and, possibly, its reduction or suppression. Once again, the prestressing of the damper can compensate the progressive deformation (SMA creep) associated to working cycles. However, as said above, in a Cu-based alloy, the progressive appearance of stabilized martensite without retransformation destroys gradually the pseudoelastic effect and the applicability of the alloy for a large number of cycles. Furthermore, for a NiTi alloy, the dynamic effects of stress and temperature and

pauses between series of cycles cannot be avoided, and therefore requires larger experimental analysis. This study, with an experimental approach, is centered on the fatigue-life analysis for a Cu-based alloy (i.e., CuAlBe) and for a NiTi alloy and, also, the aging effects of both alloys. The CuAlBe alloy is used after an appropriate heat treatment reducing the SMA creep associated to cycles, ensuring that the damper length remains "invariant" in service. Furthermore, the SMA creep in NiTi needs to be minimized to ensure a sequence of a high number of cycles without relevant increase of the length of the SMA component.

2. Experimental

The experimental analysis is focused on two SMA alloys. The CuAlBe alloy was furnished first by the research center of Trefimetaux (in 2003 and 2004) and later by NIMESIS, France (in 2005-2007) with similar original casts. For the cast AH140, the reference data are: $Ms = 255$ K; $Mf = 226$ K; $As = 253$ K; $Af = 275$ K with the following chemical composition in mass percent: Al = 11.8; Be = 0.5; Cu = 87.7. The wire from the cast AH140 of CuAlBe shows a Clausius-Clapeyron coefficient near 2.2 MPa/K (Ref 11). Several lengths of wires are used in the testing, with diameter of 3.4 mm. The CuAlBe alloy in the "as furnished state" made by direct extrusion of the wires is a mixture of phases $\alpha + \beta$ with easy progressive and permanent residual deformation that permits plastic deformation without pseudoelastic behavior. Practical application of the alloy requires a homogenization (or betatization) process. In this case, the following thermal treatment was used: heating to temperatures of 1123 K or of 1093 K, for a duration of 10 or 40 min, ensuring that the beta (bcc) phase was reached. After this annealing, the specimen was quenched in water at room temperature (i.e., 293 K). The mean grain size was 0.58 mm for 40 min at 1123 K. Further, long aging of 1 month at 373 K, and eventually, also, one additional month (or more) at 333 K

were found useful to improve the stability of the material (Ref 12) as indicated in the Fig. 5 (see below). This aging process induces a slow decrease in the CuAlBe Ms temperature.

The NiTi alloys, in the pseudoelastic state, were ordered from the SAES Getters Co. (old furnisher: Special Metals, New Hartford, NY). These alloys normally show an excellent reproducible pseudoelastic behavior from one to other sets of samples for different furnishers, and we used the wires as arrived. Two diameters were used (0.5 and 2.46 mm). In the wires of 0.5 and in 2.46 mm of diameter, the alloy was furnished in black oxide and in light oxide surfaces, respectively, with nominal As temperatures of 248/247 K and 243 K, respectively. The nominal compositions are, respectively, Ni 55.95 wt.% and 55.92 wt.% with balance in Ti. The microstructure of the NiTi wire was studied by transmission electron microscopy. A Philips CM200 LaB6 microscope was used. The crystallographic orientation of the grains is textured along the $\langle 111 \rangle$ direction (Fig. 2, left). The weakness of the 001 and the 200 type reflections indicates that the wire is textured along the $\langle 111 \rangle$ direction. The microstructure of NiTi appears in the form of small grains and subgrains with a minimum size of about 80 nm (Fig. 2, right). In addition, some precipitates of TiC and Ni3Ti2 (not visible in the figure) were observed.

The main part of measurements was performed using two "Universal Testing Machines", one is an INSTRON, model 5567 with temperature chamber 3119-005 operating between 200 and 373 K with one load cell of 30 kN and, the other is a MTS 810 with load cell of 100 kN. Eventually, the MTS uses a home-made furnace for lower temperatures (i.e., up to 373 K).

2.1 Fatigue Analysis (CuAlBe and NiTi)

The Fig. 3 shows the fracture-life for CuAlBe (left) and for NiTi (as furnished) (right). The results for CuAlBe are highly dependent on the heat treatment. The measurements indicate that true strains (when the permanent deformation or SMA
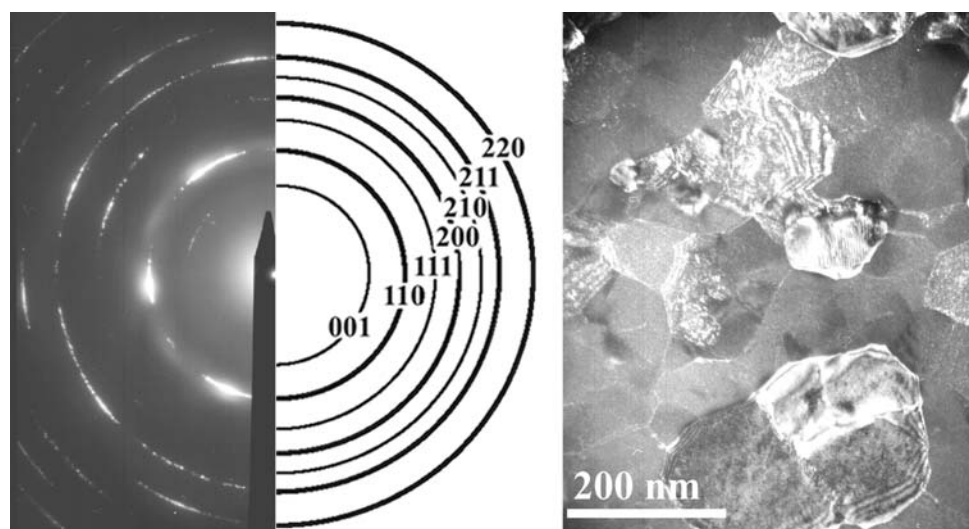

Fig. 2 Left: Electron diffraction pattern of the NiTi wire along the wire axis. Right: Dark field image taken with a small part of the 110-type ring at left
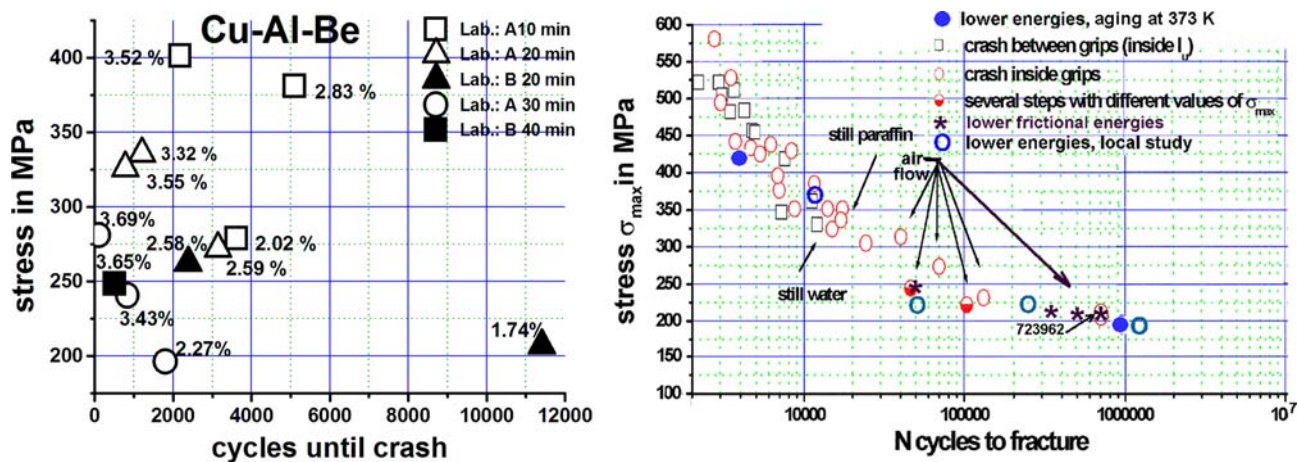

Fig. 3 Left: Fatigue and fracture behavior for CuAlBe. Wires with 3.4 mm of diameter and cycling at 0.5 Hz are used. Right: Fatigue and fracture for NiTi wire of 2.46 mm of diameter. The measurements on CuAlBe relate different length in time for the betatization process (10, 20, 30, 40 min realized in two laboratories A [Barcelona] and B [Bariloche])
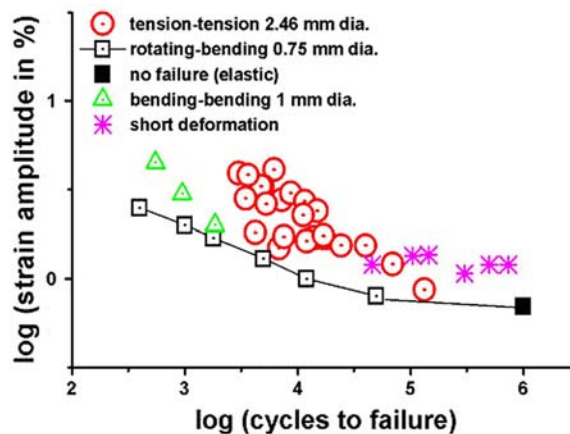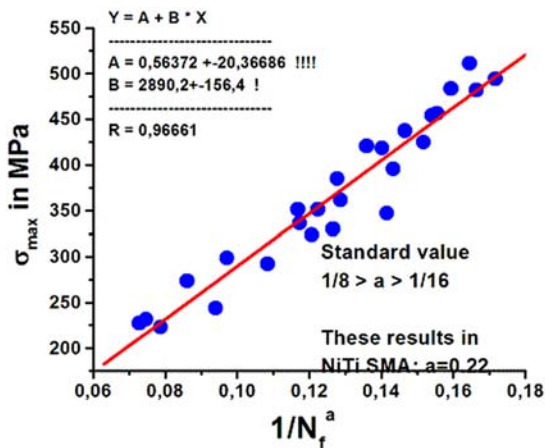
creep is subtracted) ranging from 2% to 3% and homogenization at 10 min at 1093 K produces wires which support more than 2000 working cycles, appropriate for earthquake dampers. On the other hand, the fatigue life for NiTi in cycles with only tensile stress (without bending or compression) is a function of the deformation (or the stress). Improved results (overcoming 500000 cycles) relates to lower stresses close to 200 MPa associated with lower deformation or reduced hysteresis area. In NiTi, no significant differences for rupture in grips or in free part of the sample are visualized in Fig. 3, right. Some tests using water or paraffin baths were used to diminish the overheating of the sample, but in reduced deformation, the self-heating is practically irrelevant.

The Basquin law establishes a phenomenological relation between the stress and the fatigue life via the number of cycles to failure, N_f. The law states that

$$\sigma_{\text{MAX}} = A + B^* \left(\frac{1}{(N_f)^a} \right)$$

A set of measurements is presented in Fig. 4, left. In the appropriate coordinates, the experimental measurements fit,

approximately, with the Basquin law. The value of the calculated exponent (*a*) is close to 0.22, which is clearly greater that the classical value (situated between 1/8 and 1/16). In fact, the fatigue measurements are associated to non-classical phenomena: a martensitic transformation. The Fig. 4, right, shows a comparison with results of fatigue in the Ref 13 and 14.

2.2 Aging: Time and Temperature Effects (CuAlBe and NiTi)

The main part of the analysis is done with electrical resistance and partially with stress-strain measurements in comparison with calorimetric measurements extracted from references. The Fig. 5 shows results from the CuAlBe alloy. On the left, the shape of the resistance measurements near the transformation corresponding to three different times (a, b, and c) are presented. When the aging temperatures are similar, after sufficient time, the resistance cycles are practically coincident (a and b). From the difference between a and c cycles the Ms changes after temperature changes can be obtained. The Fig. 5, right, shows the "recoverable" path induced by the aging. The Ms is a well-determined value associated to the aging

Fig. 4 Experimental data and fit via the Basquin Law (left). Right: comparison with data existing in the Ref 13 and 14 with more complex stresses
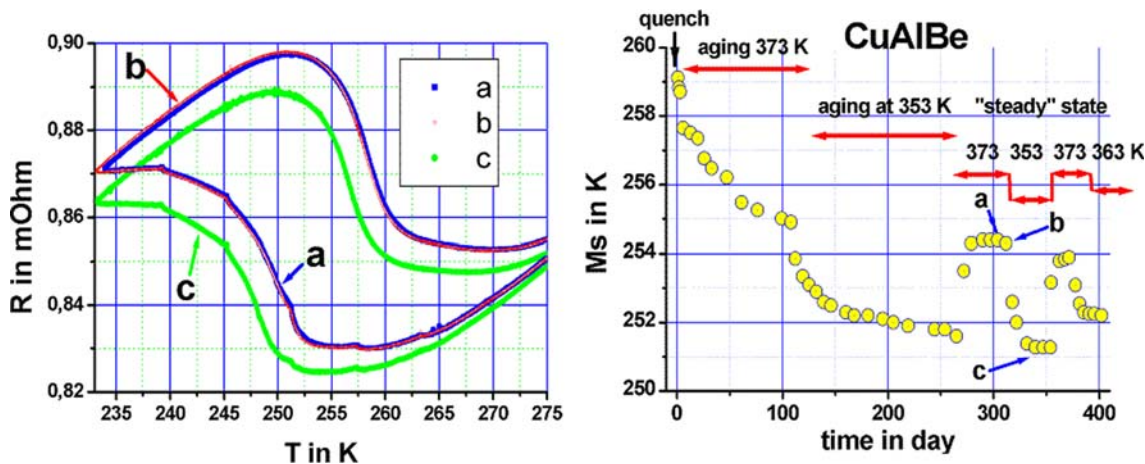
Fig. 5 Hysteresis cycle evolution due to aging determined from measurements of resistance against temperature and time. Left: Hysteresis cycle in resistance against temperature (after aging at 373 K (a and b), and at 353 K (c)). Right: Ms evolution against time after quench and further aging at different aging temperature (373, 353, and 363 K). The points (a), (b), and (c) correspond to the cycles in the left part of the figure

temperature in "steady" conditions. The Fig. 6 shows the resistance measurements associated to the R-phase transformation in NiTi. The evolution of the Rs against the aging temperature (under 800 days at 373, 388, and 398 K) is clearly visualized. The state reached after ageing does not reverse when lowering the temperature from 388 or 398 to 373 K. As a matter of fact, the Rs value increases monotonically.

The resistance measurements (as the calorimetric measurements, (Ref 9)) furnish the effect of aging on the Rs temperature. The effect of aging in NiTi is clearly different from that of the CuAlBe aging. In the Cu-based alloys, the transformation temperature (Ms) is a function of the aging temperature (after sufficient time, for steady state). In fact, the measurements indicate that the Ms tracks the room temperature evolution (Ref 8) as shown in the right part of the Fig. 5. In other words, the aging temperature induces "recoverable" effects in Ms. In NiTi, the aging effect on the R-phase transformation is much slower, but is clearly irreversible.
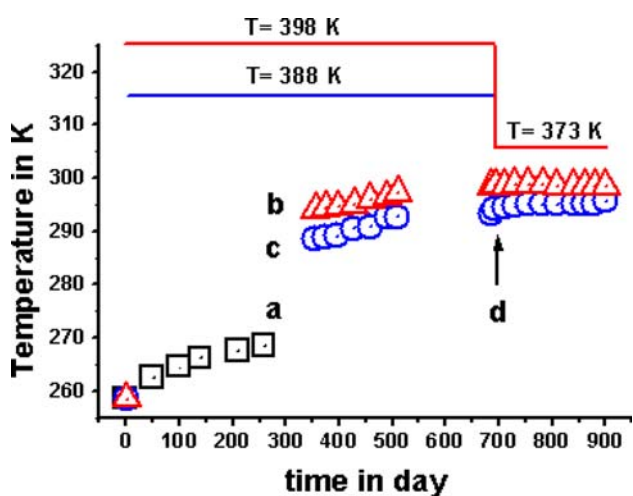

Fig. 6 Evolution on aging of the Rs temperature in NiTi alloy. Aging temperatures: 398 K for b curve, 388 K for c curve, and 373 K for a curve. After the point d, the higher temperatures were reduced to 373 K

2.3 NiTi Aging Effects on Loading

We measured the stress effect in the coexistence zone for different times at room temperature for eventual comparison with the Cu-based alloys (Ref 8). Furthermore, we measured the step obtained in the coexistence zone when a pause is imposed in an intermediate point of the "transformation plateau" (wires of 0.5 mm of diameter were used), and a subsequent cycle is performed, as indicated in Fig. 7, left. We show two consecutive measurements of the stress-strain hysteresis cycles at room temperature: the first one corresponds to the cycle with the pause in the coexistence zone for 27 days, and the second one is the immediate following cycle after the first one was completed. In Fig. 7, right, the part of the stress step is amplified to see that the global increase, including the stress reduction in the martensitic part of the sample, reaches 35 MPa, after one month of pause. The value is associated to two contributions: one part (20 MPa) is due to an increase of the transformation stress in the part of the sample that remained in parent phase. This means that the martensite initial temperature of Ms has decreased, and is more difficult to transform to martensite. The second one, 15 MPa, corresponds to a decrease of the necessary stress to maintain the transformation in the existent martensite phase. The global increase is then

$$\Delta\sigma_{tot} = \Delta\sigma_\beta + |\Delta\sigma_m|$$

We found that the variation of the necessary stress to continue the transformation when the pause is applied for one month in the coexistence zone increases with time and can reach a few tens of MPa. It is a minor effect for one month, but for longer durations (10, 20 years in prestressing for the application of SMA in earthquakes), it requires further deep study, or always avoiding the prestress.

Aging at 373 K for two months induces relevant changes in the force-deformation cycles in comparison with samples used "as furnished". The effect of aging induces a relevant reduction (35%) in the transformation stress after 100 cycles at 0.01 Hz and an increase of the hysteresis area. The experimental observations are clearly observed in Fig. 8.

The monotonic effect on Rs (Fig. 6) seems probably induced by a minor effect of precipitates associated to the lengthy aging. In Fig. 8, a decrease of the critical stress after
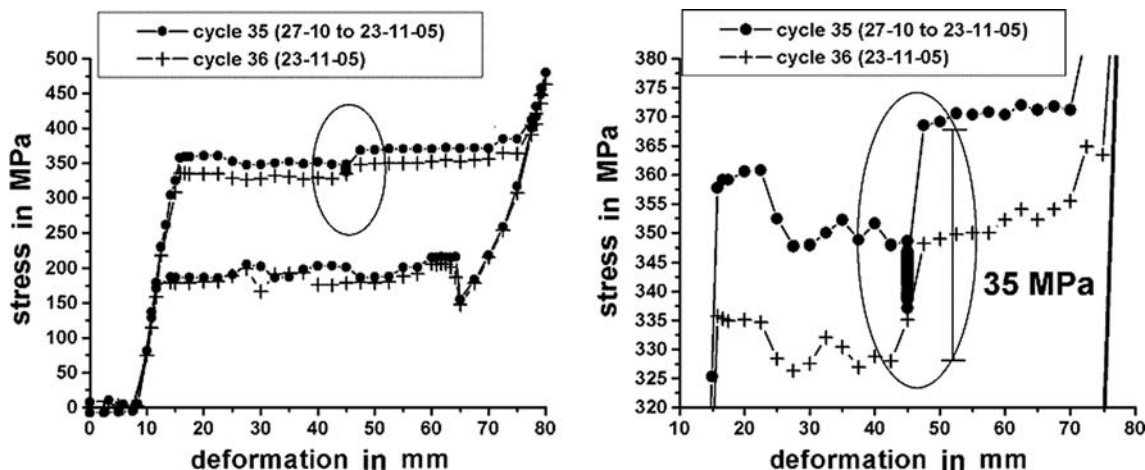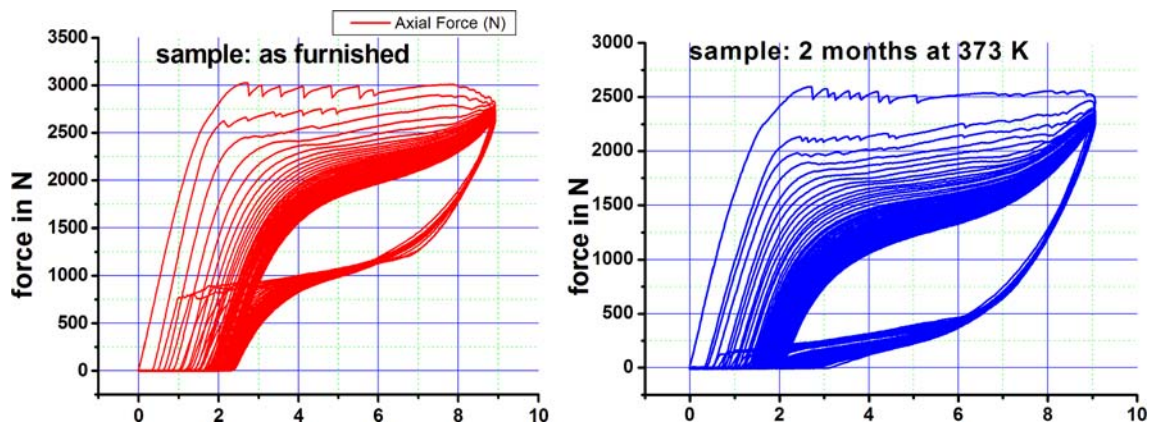

Fig. 7 Left: Two consecutive hysteresis cycles at room temperature (293 K), the first one obtained by applying a prestress in the coexistence zone for 27 days, and the immediate following one. Right: Global increase of 35 MPa ($\Delta\sigma_{tot}$) to be able to continue the cycle

Fig. 8 Hysteresis cycles for NiTi of 2.46 mm of diameter, 100 cycles at 0.01 Hz (useful samples length close to 106.5 mm). Left: Sample as furnished, Right: sample after two months at 373 K
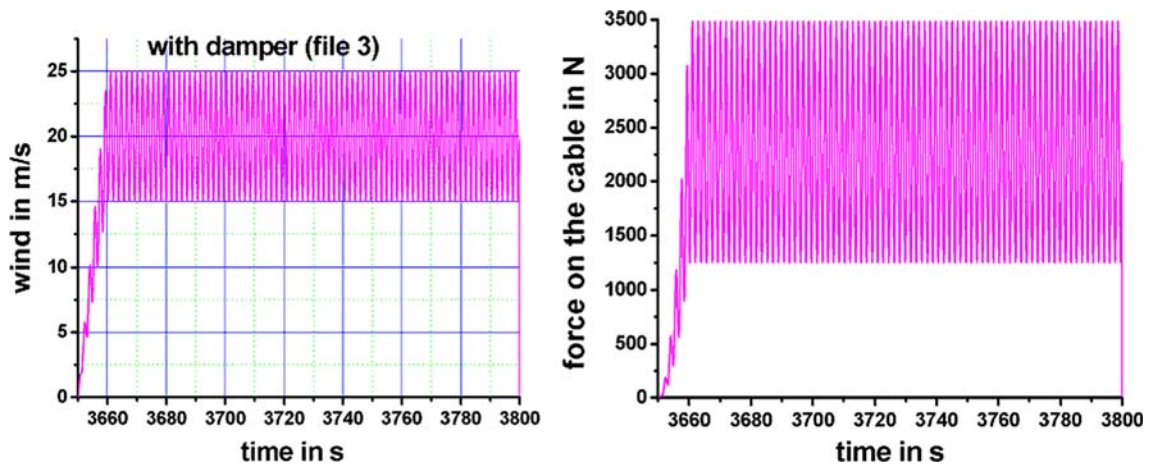
Fig. 9 Left: Periodic wind action on the cable in m/s. Right: Force on the cable in N

100 cycles is also observed for the aged samples (two months at 373 K). The effect seems coherent with the Rs extracted from resistance measurements. See, for instance, similar effects induced by the precipitates in CuZnAl in Ref 15.

The results obtained form stress-strain representation shows some differences in comparison with calorimetric or resistance measurements of the aged samples (Ref 9). The differences between resistance against temperature and force-deformation can be associated to the different characteristics of the used thermodynamic forces: (1) the temperature is one scalar thermodynamic force that does not induce relevant shape change in the transformation cycles and (2) the force induces relevant shape change by the oriented martensite variants and the privileged transformation direction.

2.4 The SMA as Dampers

The positive effects of CuAlBe in dampers for a family house are described in Ref 16. The damping actions of NiTi for the stayed cables in the Iroise bridges and in the ELSA cable 1 facility are partly investigated in this article. Using the ANSYS code, several simulations were performed using appropriate proprietary routines for the SMA behavior. The analysis is centered in only one cable of the bridge. A sinusoidal wind is

simulated (Fig. 9, left) acting on the cable with one periodical force to induce oscillations (Fig. 9, right).

The Fig. 10 includes the amplitude evolution in free and damped cable (left) and the kinetic energy in the cable free and damped. It also includes the energy absorbed by the damper and transformed to heat. The left part of Fig. 10, left, shows the displacement for free cable, with progressive increase of amplitude. The right part of Fig. 10, left, visualizes the amplitude reduction and some beats when NiTi SMA damper is introduced in simulation. The Fig. 10, right, shows the energies in the cable. At left, progressive increase of kinetic energy in the undamped cable; right curve: kinetic energy under the combined effects of wind and damper. The line "mechanical to heat" shows the monotonic growth of the energy absorbed by the damper.

One experimental analysis of effectiveness of the NiTi SMA is realized using the cable 1 in the ELSA-JRC facility. The cross-sectional area of the steel inside the cable is 7×10^{-4} m², the tension on the cable is 250 kN, and the free oscillation frequency is 1.8 Hz. Since the cable is covered by wax, spontaneous damping of oscillations appears before the SMA device is connected. In this case, a minimal scaling in external actions and in SMA wires is necessary to account for the differences in, for instance, length and cross section. The selected Iroise cable has an external diameter, length, and mass
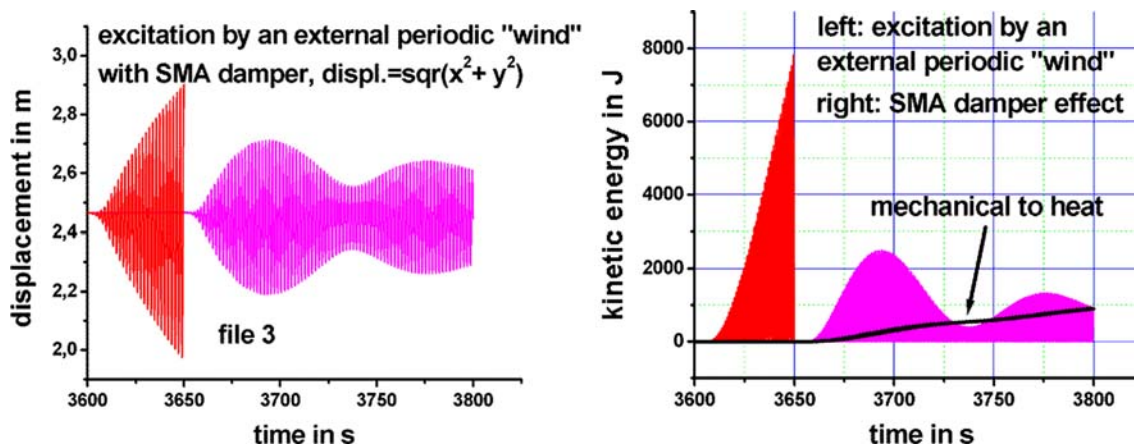
Fig. 10 ANSYS simulation: Effects on the Iroise cable. Cable without damper (outline bottom) and cable with SMA damper (outline top) figures displaced in time in order to compare. Left: Oscillation amplitude (at left) for free cable with progressively increasing amplitude. The right part shows the amplitude reduction, and some beats when NiTi SMA damper is introduced in simulation. Right: Energies in the cable. The continuous line indicate by the arrow corresponds to dissipated energy by the SMA damper
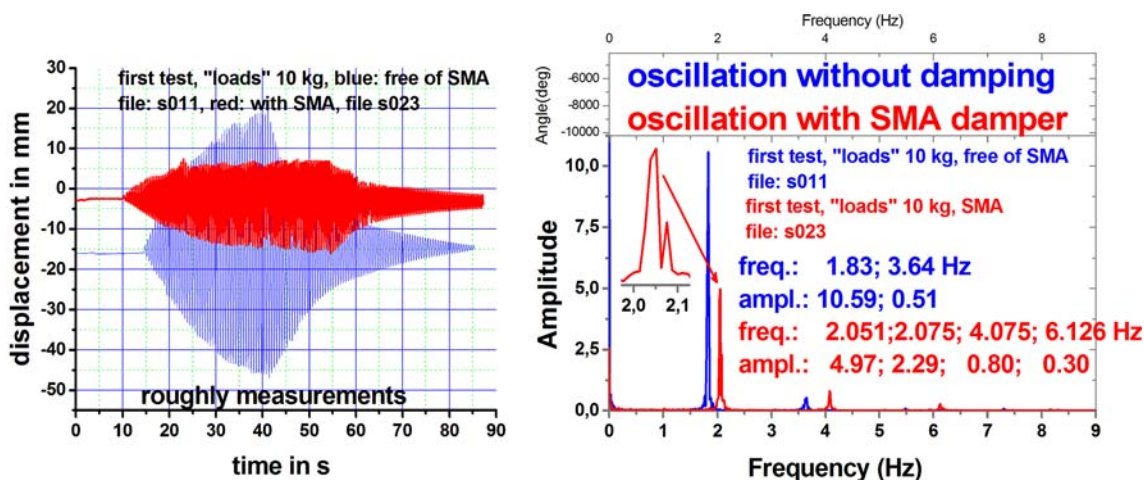
Fig. 11 Effects on the ELSA cable when a periodic excitation (amplitude close to 100 N) associated to resonant frequency is used. Left: Oscillations when there is no SMA (blue). With SMA (red), oscillations appear with reduced amplitude (near 1/3 of the amplitude oscillations in free conditions). Right: Frequency analysis of the experimental data

of 18 cm, 172 m, and 79.6 kg/m, respectively, and is subjected to 5.2 MN of tension. The ELSA cable has around 8 cm of external diameter, 45 m of length, and the mass 9 kg/m, and is subjected to 250 kN of tension. Two types of actions are realized on the ELSA cable, periodic force (near 100 N) to increase the amplitude without, and with only one SMA wire, Fig. 11 (left, displacement, and right, frequency analysis). The SMA wire (length 414 cm), is previously "trained" via a mechanical treatment of 100 cycles at 0.01 Hz corresponding to cycles as shown in Fig. 8, left. The damper is situated perpendicular to the cable at ¼ of their length. The frequency analysis shows that the oscillations occur at resonance frequencies, and then the decrease in amplitude is directly related to an increased damping. Their action induces minor changes in the oscillation frequency as shown in the Fig. 11, right. The frequency analysis using the Fast Fourier Transform of displacements against time shows that without the SMA, the main frequency is always close to 1.8 Hz, and that with SMA damper, the main frequency increases by a 10% and splits in two close frequencies near 2.05 Hz inducing eventual beats in

the oscillations (as shows the Fig. 10). The results determined by simulation are similar to those of the experimental measurements.

3. Remarks and Conclusions

This study analyzed the fatigue behavior of a CuAlBe SMA alloy, showing that while it is appropriate for damping in Civil Engineering against the effects of earthquakes, it is not well suited in the actual state of the art, for continuous, long fatigue life. However, some experiments about the performance of a NiTi alloy show that this alloy could indeed be suitable for their eventual application to damping of stayed cables.

For one or two minutes of induced oscillations at 1 Hz, the fatigue life for CuAlBe is sufficient for damping the earthquakes effect; the action of strong winds and rain associated to strong storms (several days) requires around 500000 cycles of work, and the NiTi is more appropriate for this job.

Recoverable against nonrecoverable long-time aging effects in CuAlBe and in NiTi can be observed using, for instance, electrical resistance-temperature cycles. The effect on Ms (CuAlBe) and on Rs (NiTi) can be associated, respectively, to effects of vacancy concentration (tracking between the Ms and the external room temperature) and minor precipitation. The different behavior of the alloys motivates different choices for different applications, as earthquake effects mitigation (large waiting durations, few cycles of activity), or damping of oscillations induced by wind in cables (nearly immediate action, long-fatigue life needed).

The analysis of the simulation of damper behavior in stayed cable shows satisfactory behavior: the relevant reduction of amplitude to less than one half. The experimental observations indicate an increase of cable damping, and are coherent with the calculated values. In order to optimize the action of SMA damper, deeper study of the frequencies changes with the damper loads seems necessary.

References

1. K. Otsuka and C.M. Waymann, Ed., *Shape Memory Materials*, Cambridge Univ. Press, Cambridge, 1998

2. V. Torra, A. Isalgue, and F.C. Lovey, Microstructure and Thermodynamics of the Martensitic Transformation, *Can. Metall. Quart.*, 2000, **39**, p 207–216

3. H. Janocha, Ed., *Adaptronics and Smart Structures*, Springer-Verlag, Berlin, 1999, p 334–369

4. J. Salichs, Z. Hou, and M. Noori, Vibration Suppression of Structures Using Passive Shape Memory Alloy Energy Dissipation Devices, *J. Intell. Mater. Syst. Struct.*, 2001, **12**, p 671–680

5. J.C. Wilson, M. Eeri, and M.J. Wesolowsky, Shape Memory Alloys for Seismic Response Modification: A State of the Art Review, *Earthquake Spectra*, 2005, **21**, p 569–601

6. C. Auguet, A. Isalgue, F.C. Lovey, F. Martorell, and V. Torra, Metastable Effects on Martensitic Transformation in SMA Part IV: Thermomechanical Properties of CuAlBe and NiTi Observations for Dampers in Family Houses, *J. Thermal Anal. Calorim.*, 2007, **88**, p 537–548

7. V. Torra, A. Isalgue, C. Auguet, F.C. Lovey, J.L. Pelegrina, and P. Terriault, Pre-stressed NiTi: Effects of the Thermodynamic Forces and Time, *Proceedings of the International Conference on Shape Memory and Superelastic Technologies* (Tsukuba, Japan), S. Miyazaki, Ed., ASM International, OH, 2007, p 195–203. ISBN: 978-0-87170-722-2

8. V. Torra, J.L. Pelegrina, A. Isalgue, and F.C. Lovey, Metastable Effects on Martensitic Transformation in SMA (I): Recoverable Effects by the Action of Thermodynamic Forces in Parent Phase, *J. Thermal Anal. Calorim.*, 2005, **81**, p 131–135

9. C. Auguet, A. Isalgue, F.C. Lovey, J.L. Pelegrina, S. Ruiz, and V. Torra, Metastable Effects on Martensitic Transformation in SMA. Part III. Tentative Temperature Effects in a NiTi Alloy, *J. Thermal Anal. Calorim.*, 2007, **89**(2), p 537–542

10. A. Isalgué, F.C. Lovey, P. Terriault, F. Martorell, R.M. Torra, and V. Torra, SMA for Dampers in Civil Engineering, *Mater. Trans.*, 2006, **47**, p 682–690

11. A. Isalgue, V. Torra, A. Yawny, and F.C. Lovey, Metastable Effects on Martensitic Transformation in SMA. Part VI. The Clausius-Clapeyron Relationship, *J. Thermal Anal. Calorim.*, 2008, **91**(3), p 991–998

12. A. Isalgue, J. Fernandez, V. Torra, and F.C. Lovey, Conditioning Treatments of CuAlBe SMA for Dampers, *Mater. Sci. Eng. A*, 2006, **438–440**, p 1085–1088

13. H. Tobushi, T. Hachisuka, S. Yamada, and P.-H. Lin, Rotating-bending Fatigue of a NiTi Shape Memory Alloy Wire, *Mech. Mater.*, 1997, **26**, p 35–42

14. M.G. de Azevedo, R. Fonseca, and V.T. Lopes, The Influence of High Amplitude Cycling Straining on the Behaviour of Superelastic NiTi, *Int. J. Fatigue*, 2006, **28**, p 1087–1091

15. F.C. Lovey and V. Torra, Shape Memory in Cu-based Alloys: Phenomenological Behavior at the Mesoscale Level and Interaction of Martensitic Transformation with Structural Defects in Cu-Zn-Al, *Prog. Mater. Sci.*, 1999, **44**(3), p 189–289

16. V. Torra, A. Isalgue, F. Martorell, P. Terriault, and F.C. Lovey, Built in Dampers for Family Homes via SMA: An ANSYS Computation Scheme Based on Mesoscopic and Microscopic Experimental Analyses, *Eng. Struct.*, 2007, **29**, p 1889–1902